







RESEARCH ARTICLE | JANUARY 04 2023

Polarization switching dynamics simulation by using the practical distribution of ferroelectric properties

Cheol Jun Kim ; Jae Yeob Lee ; Minkyung Ku; Seung Won Lee ; Ji-Hoon Ahn ; Bo Soo Kang  

 Check for updates

Appl. Phys. Lett. 122, 012901 (2023)

<https://doi.org/10.1063/5.0131087>



Boost Your Optics and Photonics Measurements



Lock-in Amplifier



[Find out more](#)

Boxcar Averager

Polarization switching dynamics simulation by using the practical distribution of ferroelectric properties

Cite as: Appl. Phys. Lett. **122**, 012901 (2023); doi: 10.1063/5.0131087

Submitted: 18 October 2022 · Accepted: 18 December 2022 ·

Published Online: 4 January 2023






View Online



Export Citation



CrossMark

Cheol Jun Kim,¹  Jae Yeob Lee,²  Minkyung Ku,²  Seung Won Lee,³  Ji-Hoon Ahn,³  and Bo Soo Kang^{2,a)} 

AFFILIATIONS

¹Department of Applied Physics, Center for Bionano Intelligence Education and Research, Hanyang University, Ansan 15588, South Korea

²Department of Applied Physics, Hanyang University, Ansan 15588, South Korea

³Department of Materials Science and Chemical Engineering, Hanyang University, Ansan 15588, South Korea

^{a)}Author to whom correspondence should be addressed: bosookang@hanyang.ac.kr

ABSTRACT

We investigated the internal bias field and coercive field in a typical ferroelectric thin-film capacitor and simulated polarization switching dynamics using Euler's method. The simulation results agreed well with the experimental results and reflected the well-known polarization domain switching model in which the polarization switching occurs on the order of nucleation, growth, and coalescence. The fit parameters (damping parameters affecting the polarization change rate) also followed a certain distribution. When the expected value was used instead of full distribution, the simulation results did not agree well with corresponding experimental results. The simulation results suggested no domain structure in the polarization switching dynamics, indicating that the polarization domain structure was affected by the distribution of the fit parameters. Our results demonstrate the possibility of simulation using realistic distribution of ferroelectric properties.

Published under an exclusive license by AIP Publishing. <https://doi.org/10.1063/5.0131087>

Polarization switching dynamics in ferroelectrics is important owing to their applications in nonvolatile memory devices and negative capacitance devices. Hoffmann *et al.* simulated the polarization domain switching dynamics of a ferroelectric $\text{Pb}(\text{Zr}_{0.2}\text{Ti}_{0.8})\text{O}_3$ capacitor by modeling the capacitor as a two-dimensional plane.¹ Using this numerical approach allowed us to visually investigate the resultant dynamics. Meanwhile, ferroelectric hafnia has recently attracted much interest as a potential candidate material for various ferroelectric devices. Hafnia thin films have been fabricated using different methods and under different conditions and have shown diverse ferroelectric properties.^{2–14} Regarding the ferroelectric hysteresis loops, the distribution of the internal bias and the coercive fields is often represented by the distribution of switching densities over the film area.¹⁵ In ferroelectric polarization switching dynamics, it is important that the simulations reflect these distributions. However, the existing simulation study is performed by employing the modeled distribution of free energy coefficients and internal bias fields without harnessing the measured local properties.¹ Our proposed simulations capture these realistic material properties. Therefore, we measured the switching density and simulated the polarization switching dynamics using these results.

In this Letter, the voltage transient across a ferroelectric $\text{Hf}_{0.6}\text{Zr}_{0.4}\text{O}_2$ (HZO) thin-film capacitor was simulated using the Landau–Ginzburg–Devonshire (LGD) theory and the Landau–Khalatnikov (L–K) equation.¹ The simulation parameters were obtained from the measured values of the local internal bias and local coercive fields using first order reversal curves (FORCs) method. The simulation results agreed well with the measurement results for a certain range of the damping parameter values in the L–K equation.

A ferroelectric thin film (HZO; thickness, 9.7 nm) was grown on a TiN-coated Si substrate using atomic layer deposition. The TiN top electrode was deposited by sputtering with a shadow mask. The top electrode was square-shaped (a side length, approximately 100 μm). For crystallization, the sample was annealed at 600 °C for 1 min at 4–5 Torr atmospheric pressure in a nitrogen atmosphere, using a rapid thermal process.

The hysteresis loop of the sample was measured by applying a one-cycle triangular wave (amplitude, 3 V; frequency, 1 kHz) to the capacitor, using a Radiant Technologies Precision LC II ferroelectric tester. All measurements were performed after the previous application of the triangular wave for 10 s using the ferroelectric tester.

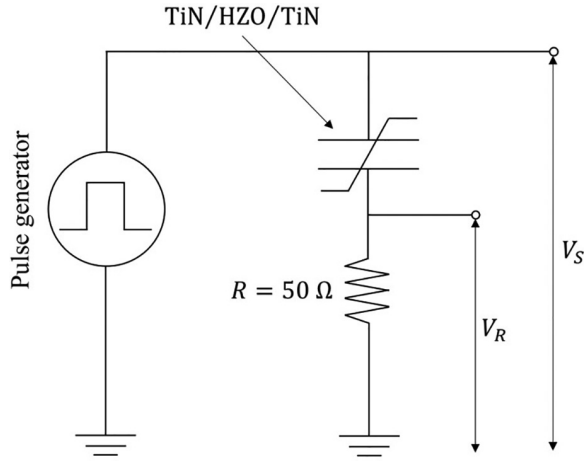


FIG. 1. Schematic of the measurement circuit.

The voltage across the ferroelectric thin-film capacitor during polarization switching was measured using the measurement circuit shown in Fig. 1. A ferroelectric capacitor and oscilloscope (input impedance, $50\ \Omega$) were connected in series. A voltage pulse was applied using a Tabor Electronics WW1071 pulse generator. First, a square pulse (height, $-3\ \text{V}$; width, $2\ \mu\text{s}$) was applied to pole the capacitor. After $20\ \mu\text{s}$, a one-cycle square wave was applied (amplitude, $3\ \text{V}$; period $4\ \mu\text{s}$). The voltage of the pulse generator V_S was directly probed using a Tektronix MDO4104C digital oscilloscope. The voltage across the ferroelectric capacitor V_F was obtained as $V_F = V_S - V_R$, where V_R was the voltage across the input impedance connected to the capacitor in series.

The switching density $\rho_{\text{SW}}(E, E_r)$ was obtained from the following equation by fitting the polarization $P(E, E_r)$ data measured using the ferroelectric tester using FORCs method, where E_r is the reversal field.¹⁵

$$\rho_{\text{SW}}(E, E_r) = -\frac{1}{2} \frac{\partial^2 P(E, E_r)}{\partial E \partial E_r}. \quad (1)$$

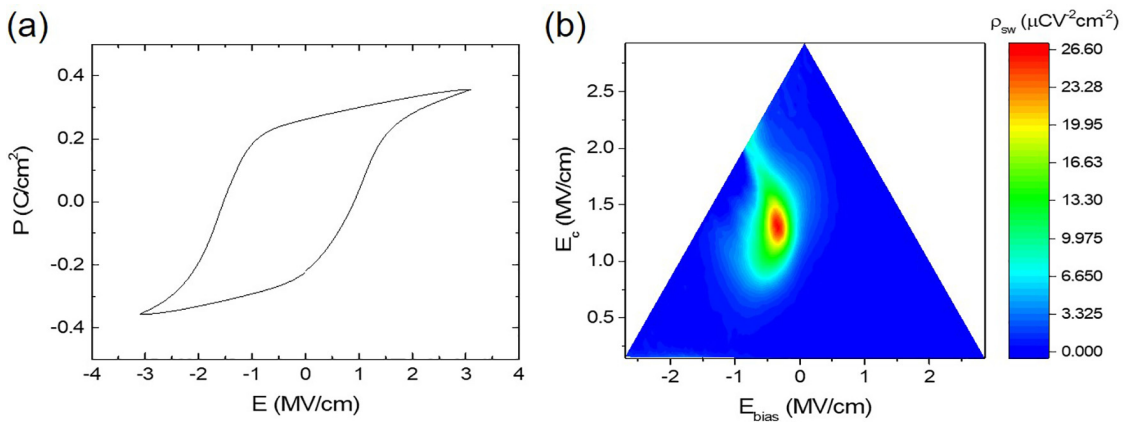


FIG. 2. (a) Hysteresis loop. (b) Distribution of switching densities.

The polarization curves were obtained from various applied electric field E sweeps from E_r to the maximal electric field E_{max} , where E_r was varied from E_{max} to $-E_{\text{max}}$. This was translated into $\rho_{\text{SW}}(E_{\text{bias}}, E_c)$ using Eq. (2), where E_{bias} and E_c are the internal bias and coercive fields, respectively,¹⁵

$$E_{\text{bias}} = \frac{E + E_r}{2}, \quad E_c = \frac{E - E_r}{2}. \quad (2)$$

The hysteresis loop shifted toward the negative direction along the voltage axis, as shown in Fig. 2(a). The distribution of the switching densities was also apparent in the negative bias field in Fig. 2(b), suggesting many local hysteresis loops with different E_{bias} and E_c values in the ferroelectric thin-film capacitor. In our numerical method, the ferroelectric capacitor was assumed to be a uniform square grid of 100×100 in the x - y plane. Therefore, E_{bias} and E_c were extracted from Fig. 2(b), as explained below.

To assign all pairs of the internal bias and coercive field values to 10 000 grids, the following procedure was performed. $N(E_{\text{bias}}, E_c)$ was defined as the largest natural number below $\rho_{\text{SW}}(E_{\text{bias}}, E_c) \times n / \rho_{\text{SW,max}}$, where $\rho_{\text{SW,max}}$ was the maximal value of $\rho_{\text{SW}}(E_{\text{bias}}, E_c)$ and n was a natural number such that the sum of $N(E_{\text{bias}}, E_c)$ was 10 000. Negative $\rho_{\text{SW}}(E_{\text{bias}}, E_c)$ values were discarded. If the sum of $N(E_{\text{bias}}, E_c)$ slightly exceeded 10 000, the lowest $N(E_{\text{bias}}, E_c)$ was replaced with $N(E_{\text{bias}}, E_c) - \epsilon$ to meet 10 000, where ϵ was a small natural number.

In our pulse experiment, the effective field $E_{\text{eff},i}$ at each i th point on the grid was given by¹

$$E_{\text{eff},i} = \frac{V_F}{t_F} - E_{\text{bias},i}, \quad (3)$$

where t_F was the ferroelectric thin-film thickness and $E_{\text{bias},i}$ was the local internal bias field at each i th point on the grid. The LGD theory describes the free energy per volume of a ferroelectrics as a polynomial function of polarization P .¹ Thus, in this theoretical framework, the free energy u_i at each point i on the grid is given by¹

$$u_i = \alpha_i P_i^2 + \beta_i P_i^4 - E_{\text{eff},i} P_i + k(\nabla P_i)^2. \quad (4)$$

In Eq. (4), α_i and β_i are the ferroelectric anisotropy constants and k is the domain coupling constant that compensates for the spatial

non-uniformity of P . α_i and β_i can be obtained from remanent polarization P_r and local coercive field $E_{c,i}$. When the minimum u_i is reached, $2\alpha P + 4\beta P^3 - E_{\text{eff}} = 0$. The E_{eff} vs P curve describes the hysteresis loop without a shift from the imprint. By employing the remanent polarization value P_r , $E_{\text{eff}} = 4\beta P(P + P_r)(P - P_r) = 4\beta P^3 - 4\beta P_r^2 P$. The extrema of the equation correspond to coercive field E_c . Local extremum points of the equation are $\pm P_r/\sqrt{3}$, implying $E_c = 8\beta P_r^3/3\sqrt{3}$. A detailed derivation is provided in the [supplementary material](#) section. Therefore, α_i and β_i are given by

$$\alpha_i = -\frac{3\sqrt{3}E_{c,i}}{4P_r}, \quad \beta_i = \frac{3\sqrt{3}E_{c,i}}{8P_r^3}, \quad (5)$$

where P_r is obtained from Fig. 2(a). The L-K equation describes the dynamics of P with the damping parameter ρ .¹⁶ The parameter ρ represents the dynamic sensitivity with which the local free energy reaches its minimum. With ρ_i at each point i on the grid, the evolution of P_i is given by¹

$$-\frac{\partial u_i}{\partial P_i} = \rho_i \frac{\partial P_i}{\partial t}. \quad (6)$$

To understand the domain dynamics during polarization switching, simulation parameters k and ρ_i were fitted to the experimental data. The fitted value of the domain coupling constant k was $10^{-5} \text{ m}^3/\text{F}$ while the damping parameter ρ_i was assumed to be uniformly distributed, with a minimum of $10 \text{ } \Omega \text{ m}$ and a maximum of $590 \text{ } \Omega \text{ m}$. A good agreement was achieved as shown in Fig. 3(a). However, the results of a simulation that used $\rho_i = 300 \text{ } \Omega \text{ m}$ (mean of the uniform distribution) did not agree well with the measured data. The simulated voltage transient [Fig. 3(b)] exhibited voltage fluctuation during the capacitor charging.

Figures 4(b)–4(f) show the polarization reversal simulation results obtained assuming uniformly distributed ρ_i (with the minimum of $10 \text{ } \Omega \text{ m}$ and maximum of $590 \text{ } \Omega \text{ m}$). The white dots in Fig. 4(b) denote the domain nucleation in the initially negatively polarized blue area. Soon, the dots grow to red dots via forward domain growth as shown in Fig. 4(c). Subsequently, via sideway growth and domain coalescence in Figs. 4(d)–4(f), the capacitor turns to a positively

polarized red area. Therefore, our simulation reflects the well-known polarization domain switching model with the nucleation, growth, and coalescence processes.^{17–19}

Figures 5(b)–5(f) show the simulated polarization reversal results obtained by assuming $\rho_i = 300 \text{ } \Omega \text{ m}$ (fixed value corresponding to the mean of the uniform distribution). The blue area slowly becomes white with a polarization value of almost zero and then eventually red. It is remarkable that the simulation yielded relatively homogeneous switching without a domain structure. Uniform ρ_i suppressed the domain nucleation; consequently, the simulated voltage in Fig. 5(a) deviated from the actually measured data.

Using distributed switching densities allowed using realistic sample's parameter values in simulations that used the LGD theory. With respect to the voltage transient, the calculations were consistent with the measurement results. In addition, the polarization switching dynamics followed the well-known polarization domain switching model. However, the simulated voltage transient did not agree well with the measured data when using $\rho_i = 300 \text{ } \Omega \text{ m}$. The polarizations switched relatively homogeneously. Therefore, polarization switching through the domain structure was affected by the distribution of the damping parameters.

The LGD theory posits that the equilibrium polarization state is P_1 when the free energy function $u(P)$ is minimal at $P = P_1$. When an external electric field is applied across a ferroelectrics, $u(P)$ changes and $\partial u/\partial P$ is no longer zero but rather takes on a nonzero at P_1 . By the L-K equation, $\partial P/\partial t$ (which is the rate of the polarization change) is related to $-\rho^{-1}\partial u/\partial P$. The damping parameter ρ affects the speed with which the polarization value changes. In Ref. 16, Chatterjee *et al.* explained the polarization of HfO_2 using a charge-mass spring system, which is a nonlinear dipole oscillator. These researchers modeled polarization switching as a damped oscillator of charged particles. The polynomial terms of polarization in the free energy were obtained from the polynomial terms in the spring. The damping parameter in the L-K equation was also obtained from the damping term in the oscillator. When a constant electric field was applied to the oscillator in a static state, the time required to reach the new equilibrium state was affected by the damping term. Similarly, when an electric field was

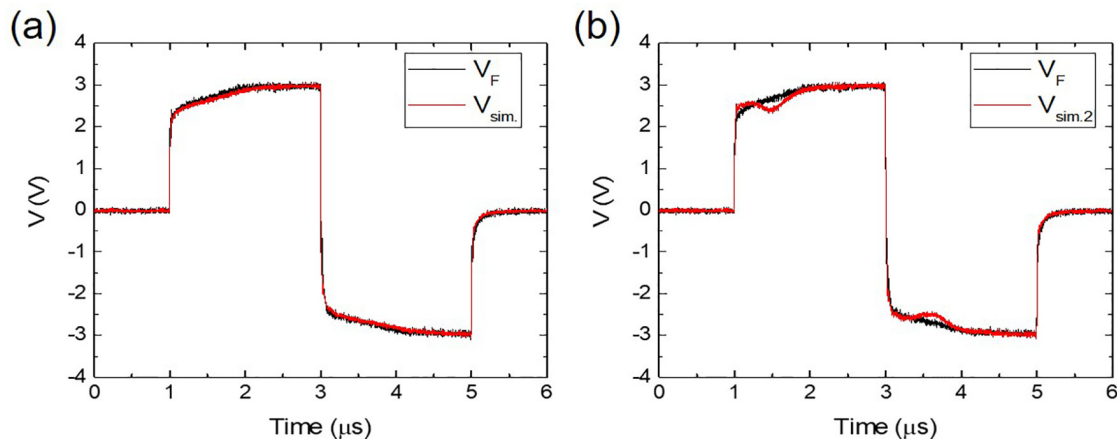


FIG. 3. The voltage transient measured across the ferroelectrics V_F and the simulated voltage transient across the ferroelectrics: (a) V_{sim} , with fitting parameters $\rho_i = 10 - 590 \text{ } \Omega \text{ m}$ and (b) $V_{\text{sim},2}$ with $\rho_i = 300 \text{ } \Omega \text{ m}$.

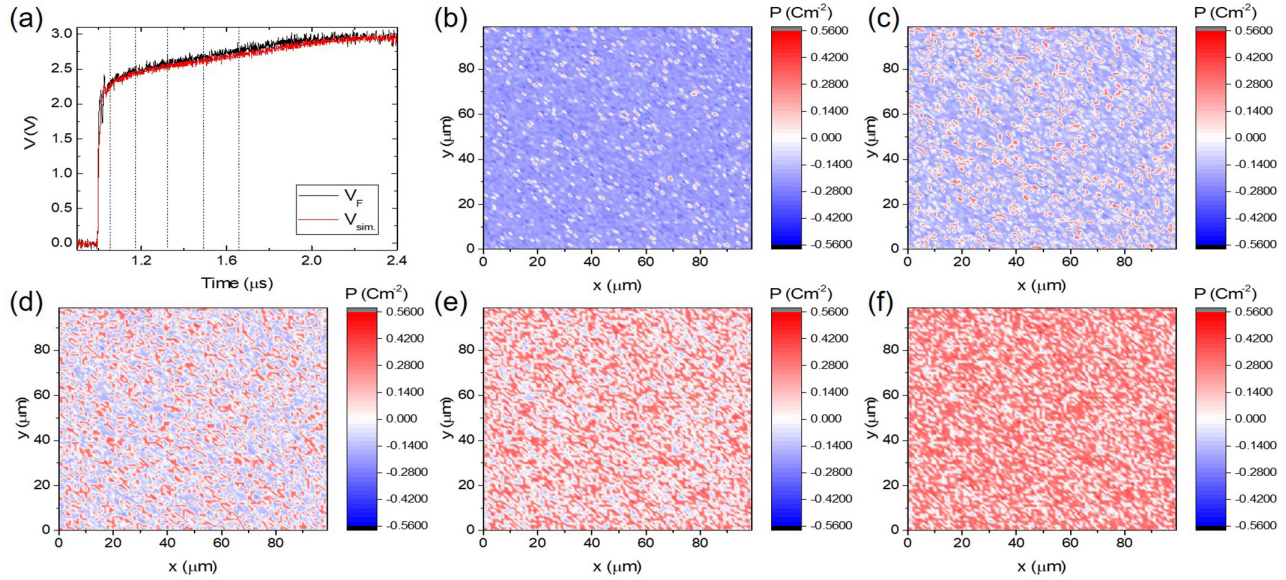


FIG. 4. (a) The simulated voltage transient across the ferroelectrics V_{sim} , with $\rho_l = 10 - 590 \Omega m$. The domain dynamics in the ferroelectric thin-film capacitor for the polarization switching in (b) 1.05, (c) 1.17, (d) 1.32, (e) 1.49, and (f) 1.65 μs .

applied across a ferroelectrics, the rate of the polarization variation was affected by the damping parameter.

Therefore, we expected similar outcomes for two simulation scenarios because 300 Ωm is the mean of the uniform distribution, with the minimum of 10 Ωm and maximum of 590 Ωm . However, these two results were different, suggesting that it is important to consider the distribution of the damping parameters. In Ref. 9, Hoffmann *et al.* prevented the immediate screening of the polarization charge during

switching for the temporary observation of the fundamentally unstable negative capacitance region without hysteresis. It was difficult to observe the region stably because homogeneous switching hardly occurred. Immediate screening owing to the charge injection induced inhomogeneous switching.²⁰ When immediate screening was prevented, the homogeneous switching was induced, and its distribution of damping parameters was the uniform distribution of a single value. With immediate screening, a well-known polarization domain

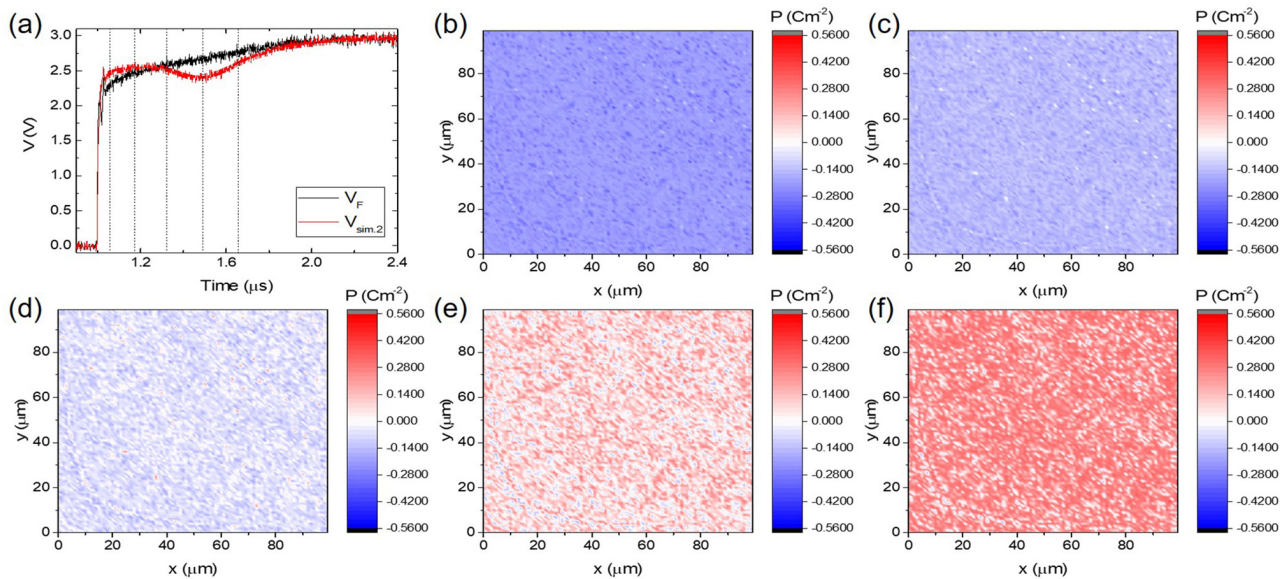


FIG. 5. (a) The simulated voltage transient across the ferroelectrics $V_{sim,2}$ with $\rho_l = 300 \Omega m$. The polarization map in the ferroelectric thin-film capacitor for the polarization switching in (b) 1.05, (c) 1.17, (d) 1.32, (e) 1.49, and (f) 1.65 μs .

switching model would become relevant, and its distribution of damping parameters would be a certain distribution with a minimum ρ and maximum ρ . Our sample's distribution of damping parameters was not a uniform distribution of a single value but a uniform distribution with a minimum ρ and maximum ρ .

In summary, we simulated the polarization switching phenomenon of a typical ferroelectric thin-film capacitor using the distributions of the switching densities. Our results show that the simulations are possible by considering the measured internal bias fields and the distribution of calculated free energy coefficients. This is important because the polarization switching dynamics is affected not only by the representative value but also by the distribution of the parameters. Also, the simulation offers the distribution of the damping parameters related to the dynamic sensitivity. We found that the distribution of damping parameters determines whether the ferroelectric polarization switching occurs by domain switching or relatively homogeneous switching. Our work can be applied in order to investigate polarization switching dynamics in the various ferroelectric materials.

See the [supplementary material](#) for the derivation of Eq. (5).

This work was supported by a National Research Foundation of Korea grant funded by the Korean Government (No. 2021R1F1A1064104). The authors would like to thank Editage (www.editage.co.kr) for English language editing.

AUTHOR DECLARATIONS

Conflict of Interest

The authors have no conflicts to disclose.

Author Contributions

Cheol Jun Kim: Conceptualization (equal); Data curation (equal); Formal analysis (equal); Investigation (equal); Methodology (equal); Project administration (equal); Software (equal); Validation (equal); Visualization (equal); Writing – original draft (equal); Writing – review & editing (equal). **Jaе Yeob Lee:** Data curation (equal); Investigation (equal). **Minkyung Ku:** Data curation (equal); Investigation (equal). **Seung Won Lee:** Resources (equal). **Ji-Hoon Ahn:** Resources (equal). **Bo Soo Kang:** Conceptualization (equal); Data curation (equal); Formal analysis (equal); Funding acquisition (equal); Investigation (equal); Methodology (equal); Project administration (equal); Resources (equal); Software (equal); Supervision (equal);

Validation (equal); Visualization (equal); Writing – review & editing (equal).

REFERENCES

- ¹M. Hoffmann, A. I. Khan, C. Serrao, Z. Lu, S. Salahuddin, M. Pešić, S. Slesazeck, U. Schroeder, and T. Mikolajick, *J. Appl. Phys.* **123**, 184101 (2018).
- ²B. Y. Kim, H. W. Park, S. D. Hyun, Y. Bin Lee, S. H. Lee, M. Oh, S. K. Ryoo, I. S. Lee, S. Byun, D. Shim, D. Y. Cho, M. H. Park, and C. S. Hwang, *Adv. Electron. Mater.* **8**, 1 (2022).
- ³M. H. Park, Y. H. Lee, H. J. Kim, Y. J. Kim, T. Moon, K. Do Kim, J. Müller, A. Kersch, U. Schroeder, T. Mikolajick, and C. S. Hwang, *Adv. Mater.* **27**, 1811 (2015).
- ⁴S. W. Lee, C. M. Kim, J. H. Choi, C. M. Hyun, and J. H. Ahn, *Mater. Lett.* **252**, 56 (2019).
- ⁵M. Hyuk Park, H. Joon Kim, Y. Jin Kim, W. Lee, T. Moon, and C. S. Hwang, *Appl. Phys. Lett.* **102**, 242905 (2013).
- ⁶J. Bouaziz, P. R. Romeo, N. Baboux, and B. Vilquin, *ACS Appl. Electron. Mater.* **1**, 1740 (2019).
- ⁷H. A. Hsain, Y. Lee, M. Materano, T. Mittmann, A. Payne, T. Mikolajick, U. Schroeder, G. N. Parsons, and J. L. Jones, *J. Vac. Sci. Technol. A* **40**, 010803 (2022).
- ⁸H. B. Kim, M. Jung, Y. Oh, S. W. Lee, D. Suh, and J. H. Ahn, *Nanoscale* **13**, 8524 (2021).
- ⁹M. Hoffmann, F. P. G. Fengler, M. Herzog, T. Mittmann, B. Max, U. Schroeder, R. Negrea, L. Pintilie, S. Slesazeck, and T. Mikolajick, *Nature* **565**, 464 (2019).
- ¹⁰T. Mittmann, M. Materano, P. D. Lomenzo, M. H. Park, I. Stolichnov, M. Cavalieri, C. Zhou, C. C. Chung, J. L. Jones, T. Szyjka, M. Müller, A. Kersch, T. Mikolajick, and U. Schroeder, *Adv. Mater. Interfaces* **6**, 1901528 (2019).
- ¹¹H. Liang, B. Zhang, Y. Guo, X. Guo, S. Ren, Y. Li, Y. Lu, and R. Lang, *Ceram. Int.* **47**, 27843 (2021).
- ¹²S. Starschich, D. Griesche, T. Schneller, R. Waser, and U. Böttger, *Appl. Phys. Lett.* **104**, 202903 (2014).
- ¹³T. Mimura, T. Shimizu, H. Uchida, and H. Funakubo, *Appl. Phys. Lett.* **116**, 062901 (2020).
- ¹⁴T. H. Ryu, D. H. Min, and S. M. Yoon, *J. Appl. Phys.* **128**, 074102 (2020).
- ¹⁵T. Schenk, M. Hoffmann, J. Ocker, M. Pešić, T. Mikolajick, and U. Schroeder, *ACS Appl. Mater. Interfaces* **7**, 20224 (2015).
- ¹⁶K. Chatterjee, A. J. Rosner, and S. Salahuddin, *IEEE Electron Device Lett.* **38**, 1328 (2017).
- ¹⁷Y. J. Kim, H. W. Park, S. D. Hyun, H. J. Kim, K. Do Kim, Y. H. Lee, T. Moon, Y. Bin Lee, M. H. Park, and C. S. Hwang, *Nano Lett.* **17**, 7796 (2017).
- ¹⁸A. K. Tagantsev, I. Stolichnov, N. Setter, J. S. Cross, and M. Tsukada, *Phys. Rev. B* **66**, 214109 (2002).
- ¹⁹J. Y. Jo, H. S. Han, J. G. Yoon, T. K. Song, S. H. Kim, and T. W. Noh, *Phys. Rev. Lett.* **99**, 267602 (2007).
- ²⁰Y. J. Kim, H. Yamada, T. Moon, Y. J. Kwon, C. H. An, H. J. Kim, K. Do Kim, Y. H. Lee, S. D. Hyun, M. H. Park, and C. S. Hwang, *Nano Lett.* **16**, 4375 (2016).